Classification

Major Category: Biological Sciences

Minor Category: Microbiology

The Evolution of Fluoroquinolone-Resistance in *Mycobacterium tuberculosis* is Modulated by the Genetic Background

Rhastin A. D. Castro[1,2], Amanda Ross[1,2], Lujeko Kamwela[1,2], Miriam Reinhard[1,2], Chloé Loiseau[1,2], Julia Feldmann[1,2], Sonia Borrell[1,2], Andrej Trauner[1,2,†], and Sebastien Gagneux[1,2,*]

[1]Swiss Tropical and Public Health Institute, Basel, Switzerland

[2]University of Basel, Basel, Switzerland

[*],[†]Corresponding authors

Socinstrasse 57, 4051 Basel, Switzerland

T: +41 61 284 6983

F: +41 61 284 8101

Email: sebastien.gagneux@swisstph.ch

Email: andrej.trauner@swisstph.ch

Abstract

Fluoroquinolones (FQ) form the backbone in experimental treatment regimens against drug-susceptible tuberculosis. However, little is known on whether the genetic variation present

in natural populations of *Mycobacterium tuberculosis* (*Mtb*) affects the evolution of FQ-resistance (FQ-R). To investigate this question, we used a set of *Mtb* strains that included nine genetically distinct drug-susceptible clinical isolates, and measured their frequency of resistance to the FQ ofloxacin (OFX) *in vitro*. We found that the *Mtb* genetic background led to differences in the frequency of OFX-resistance (OFX-R) that spanned two orders of magnitude and substantially modulated the observed mutational profiles for OFX-R. Further *in vitro* assays showed that the genetic background also influenced the minimum inhibitory concentration and the fitness effect conferred by a given OFX-R mutation. To test the clinical relevance of our *in vitro* work, we surveyed the mutational profile for FQ-R in publicly available genomic sequences from clinical *Mtb* isolates, and found substantial *Mtb* lineage-dependent variability. Comparison of the clinical and the *in vitro* mutational profiles for FQ-R showed that 45% and 19% of the variability in the clinical frequency of FQ-R *gyrA* mutations in Lineage 2 and Lineage 4 strains, respectively, can be attributed to how *Mtb* evolves FQ-R *in vitro*. As the *Mtb* genetic background strongly influenced the evolution of FQ-R *in vitro*, we conclude that the genetic background of *Mtb* also impacts the evolution of FQ-R in the clinic.

Keywords: *Mycobacterium tuberculosis*, antimicrobial resistance, evolution, fluoroquinolones, epistasis

Significance

Newer generations of fluoroquinolones form the backbone in many experimental treatment regimens against *M. tuberculosis* (*Mtb*). While the genetic variation in natural populations of *Mtb* can influence resistance evolution to multiple different antibiotics, it is

unclear whether it modulates fluoroquinolone-resistance evolution as well. Using a combination of *in vitro* assays coupled with genomic analysis of clinical isolates, we provide the first evidence illustrating the *Mtb* genetic background's substantial role in fluoroquinolone-resistance evolution, and highlight the importance of bacterial genetics when studying the prevalence of fluoroquinolone-resistance in *Mtb*. Our work may provide insights into how to maximize the timespan in which fluoroquinolones remain effective in clinical settings, whether as part of current standardized regimens, or in new regimens against *Mtb*.

Introduction

Antimicrobial resistance (AMR) poses a major threat to our ability to treat infectious diseases (1, 2). The rise of AMR is a complex phenomenon with a broad range of contributing socioeconomic and behavioural factors (3–7). However, the emergence of AMR within any pathogen population is ultimately an evolutionary process (8, 9). This evolutionary process is influenced by multiple factors, including drug pressure and pathogen genetics. Firstly, the drug type and drug concentration can affect the type and relative frequencies of AMR mutations observed in a given pathogen population (also known as the mutational profile for AMR) (9–14). Secondly, pathogen populations comprise genetically distinct strains, and this genetic variation may also influence AMR evolution (15–17). Different pathogen genetic backgrounds can have different baseline susceptibilities to a given drug (18, 19), which consequently can affect patient treatment outcomes (20). The genetic background has also been shown to modulate the acquisition and prevalence of AMR (11, 15, 21, 22), the mutational profile for AMR (11, 15, 16, 23), and the phenotypic effects of AMR mutations (24–28). Studying the interplay between

pathogen genetics and drug pressure is therefore important in understanding how to restrict the prevalence of AMR in pathogen populations.

AMR in *Mycobacterium tuberculosis* (*Mtb*), the aetiological agent of human tuberculosis (TB), is of particular importance. *Mtb* infections globally cause the highest rate of mortality due to a single infectious agent both in general, and due to AMR specifically (29). Although the genetic variation in *Mtb* is small compared to other bacterial pathogens (17, 30), several studies have shown that this limited genetic variation influences AMR phenotypes and prevalence (15, 17, 24, 28, 31). The global genetic diversity of *Mtb* comprises seven phylogenetic lineages (17, 30), and *Mtb* strains belonging to the Lineage 2 Beijing/W genetic background have repeatedly been associated with multidrug-resistant TB (MDR-TB; defined as an infection from an *Mtb* strain that is resistant to at least isoniazid and rifampicin) both *in vitro* and in clinical settings (4, 11, 15, 21, 22).

One strategy to reduce the emergence of AMR in *Mtb* is the development of new, shorter treatment regimens (32, 33). Many such experimental regimens use third- or fourth-generation fluoroquinolones (FQ) against drug-susceptible *Mtb* (32–36). However, FQs have long been integral to treating MDR-TB (37), and the previous use of FQ has led to the emergence of FQ-resistance (FQ-R) in clinical strains of *Mtb* (7, 38–40). FQ-R is one of the defining properties of extensively drug-resistant TB (XDR-TB), and XDR-TB accounts for 8.5% of MDR-TB cases (29). Understanding how FQ-R is acquired in natural populations of *Mtb* may allow for the development of tools or strategies to mitigate further increases in FQ-R prevalence.

In *Mtb*, the sole target of FQ is DNA gyrase (10, 38, 41–43). Consequently, clinically relevant FQ-R in *Mtb* is primarily due to a limited set of chromosomal mutations located within the “quinolone-resistance-determining region” (QRDR) of the *gyrA* and *gyrB* genes, which

encode DNA gyrase (22, 38, 39). No horizontal gene-transfer (HGT) or plasmid-based resistance to FQ has been documented in *Mtb* (44, 45). Studying FQ-R evolution in *Mtb* populations thus provides a promising setting for elucidating how the genetic background may affect the emergence and maintenance of clinically relevant chromosomal AMR mutations in bacterial populations.

While a great deal of literature exists on the biochemical mechanisms leading to the FQ-R phenotype in *Mtb* (10, 41–43, 46, 47), little is known on the evolutionary dynamics of FQ-R in different populations of *Mtb*. Given that antimicrobial regimens against *Mtb* infections use standardized, empirical dosing strategies (29), it is unclear whether different *Mtb* genetic backgrounds would acquire FQ-R at the same frequency when exposed to the same antimicrobial concentration. Whether the *Mtb* genetic background would also modulate the mutational profile for FQ-R, or the phenotypic effects of FQ-R mutations, is unknown. Such knowledge may provide insights on how to maintain or prolong the efficiency of FQs against different genetic variants of *Mtb* in the clinic.

In this study, we tested whether the *Mtb* genetic background plays a role in the evolution of FQ-R. Specifically, we showed that the *Mtb* genetic background can lead to differences in the frequency of FQ-R emergence that span two-orders of magnitude, as well as substantially modulate the mutational profile for FQ-R. We further demonstrated that the phenotypic effects of clinically relevant FQ-R mutations differed depending on the *Mtb* genetic background they were present in. Analysis of publicly available genomic sequences from clinical *Mtb* isolates also revealed a positive association between the FQ-R mutational profiles observed *in vitro* and the mutational profiles observed in the clinic. Taken together, we showed that the *Mtb* genetic background had a considerable role in evolution of FQ-R in the clinic.

Results

Frequency of ofloxacin-resistance in *M. tuberculosis* is strain-dependent

We first tested for whether the *Mtb* genetic background led to differences in the frequency of FQ-R acquisition. To do so, we performed a Luria-Delbrück fluctuation analysis on nine drug-susceptible and genetically distinct *Mtb* clinical strains belonging to Lineage 1 (L1), Lineage 2 (L2) and Lineage 4 (L4) (See SI Appendix, Table S1) (17, 30, 48, 49). We measured their frequency of resistance *in vitro* to the FQ ofloxacin (OFX), as OFX was used extensively to treat MDR-TB patients in the past. Given that anti-TB treatment regimens use standardized drug concentrations (29), we also measured the frequency of resistance to the same concentration of OFX (4 µg/mL) for all nine strains. We observed significant strain-dependent variation in the frequency of OFX-resistance (OFX-R) at 4 µg/mL, with the difference spanning two orders of magnitude (Fig. 1A; $P = 2.2 \times 10^{-16}$, Kruskal-Wallis). Several of the nine drug-susceptible *Mtb* strains contained missense substitutions in DNA gyrase that are not associated with FQ-R (See SI Appendix, Table S2) (49). These mutations are phylogenetic markers that reflect the population structure of *Mtb* and cannot be avoided if strains from different *Mtb* lineages are used (17, 30). We found no evidence for any associations between the presence a given phylogenetic DNA gyrase missense mutation and the frequency of OFX-R acquired.

The concentration of the antimicrobial can affect the observed frequencies of AMR in *Mtb* (10, 11, 13). Therefore, we tested whether changing the selective concentration of OFX would affect the relative differences in strain-specific OFX-R frequencies. For the sake of simplicity, we tested only two strains, with each strain at the opposite extremes of the frequency of resistance to 4 µg/mL OFX, as shown in Fig. 1A: N0157 (high OFX-R frequency) and N0145 (low OFX-R

138 frequency). We found that the frequency of OFX-R remained one to two-orders of magnitude
139 higher in N0157 than in N0145 across all the concentrations we tested (Fig. 1B, $P = 2.46 \times 10^{-5}$
140 for 2 µg/mL OFX, and $P = 4.03 \times 10^{-6}$ for 8 µg/mL OFX, Wilcoxon rank-sum test). The N0157
141 strain had nearly confluent growth at 2 µg/mL OFX, which is the OFX concentration that has
142 been shown to inhibit 95% of *Mtb* strains that have not been previously exposed to OFX, but
143 does not inhibit *Mtb* strains that are considered resistant to OFX in the clinic (18, 19). This
144 suggested that N0157 has low-level resistance to OFX, despite having no mutation in the QRDR.
145 Meanwhile, at 8 µg/mL OFX, we observed only four resistant colonies for N0145 across all
146 samples, with all colonies arising within the same culture.

147 The variation in OFX-R frequencies when selecting on the same concentration of OFX
148 may be driven by several, non-exclusive biological factors. Firstly, the *Mtb* strains we tested may
149 have different baseline DNA mutation rates. Secondly, the number and relative frequency of
150 potential mutations that confer OFX-R may vary depending on the *Mtb* genetic background.
151 Thirdly, the relative cost of OFX-R mutations may differ between *Mtb* genetic backgrounds. As
152 the observed frequency of OFX-R in *Mtb* is likely the result from a combination of multiple
153 factors, we took advantage of the fact that we had identified strains with a range of OFX-R
154 frequencies. We selected three representative strains with significantly different OFX-R
155 frequencies: N0157, N1283, and N0145. These strains had a high, mid-, and low frequency of
156 OFX-R, respectively (Fig. 1A). We then explored the relative contributions of each biological
157 factor listed above in driving the variation in OFX-R across genetically distinct *Mtb* strains.
158
159 **Mutation rate differences do not drive the *in vitro* variation in ofloxacin-resistance**
160 **frequency in *M. tuberculosis***

We first tested for the presence of differential mutation rates between our panel of *Mtb* strains in Fig. 1A. Mutations in *dnaE*, which encodes the replicative DNA polymerase and serves as the major replicative exonuclease in *Mtb*, have been shown to confer a hypermutator phenotype in *Mtb* in the absence of environmental stress (50, 51). While *dnaE* mutations were present in the genomic data of our panel of drug-susceptible *Mtb* strains (See SI Appendix, Table S2) (49), none were in the polymerase and histidinol phosphatase domain of DnaE, the region where mutations would impart a hypermutator phenotype (50, 51). We did not test for the presence of *dnaE* mutations in the resistant colonies following the fluctuation analysis, as we reasoned that the likelihood of gaining both a *dnaE* and a *gyrA* double mutation within this relatively short period is extremely low as to be considered negligible. To test for mutation rate variation *in vitro*, we again conducted a fluctuation analysis on N0157, N1283, and N0145 (the high-, mid-, and low-frequency OFX-R strains, respectively), but used streptomycin (STR; 100 µg/mL) instead of OFX. We hypothesized that if the frequency of OFX-R is driven by differential mutation rates, then we should expect similar differences in the frequency of STR-resistance (STR-R). However, we observed no evidence for differences in the frequency of STR-R between the strains tested (Fig. 2, $P = 0.135$, Kruskal-Wallis; See SI Appendix, Table S3). This suggested that the observed differences in frequency of resistance are specific to OFX, and that there are limited, if any, inherent differences in mutation rate between the *Mtb* strains tested.

Mutational profile for ofloxacin-resistance is highly strain-dependent

We next determined the mutational profile for OFX-R for each strain used in the fluctuation analysis at 4 µg/mL OFX (Fig. 1A). The QRDR mutations in 680 *gyrA* and 590 *gyrB* sequences were identified in the resistant colonies. We observed that *gyrA* mutations made up

99.7% of the QRDR mutations observed (645 *gyrA* mutations, 2 *gyrB* mutations), and no QRDR double-mutants were present (See SI Appendix, Tables S4-S5). The mutational profiles for OFX-R were also highly strain-specific (Fig. 3A, $P = 5.00 \times 10^{-4}$, Fisher's exact test). Specifically, the GyrA A90V mutation was most prevalent in the high-frequency OFX-R strains, while GyrA D94G was most prevalent in all other strains. There was also a slight trend showing that strains with a greater number of unique *gyrA* mutations present also had higher rates of OFX-R (Fig. 1A; Fig. 3B).

The strain-dependent variation the mutational profile for OFX-R may be due to *gyrA* mutations conferring different resistance levels depending on the *Mtb* strain they are present in. To test this hypothesis, we first isolated OFX-R mutants carrying one of four possible GyrA mutations (G88C, A90V, D94G, or D94N) in the three strains used in Fig. 2: N0157, N1283, and N0145. The OFX MIC was determined for each of the twelve OFX-R mutant strains, along with their respective wild-type ancestors. We found that each parental wild-type strain had different susceptibilities to OFX, with N0157, N1283, and N0145 having OFX MICs of 2 µg/mL, 0.6 µg/mL, and 0.5 µg/mL, respectively (Fig. 4A; See SI Appendix, Table S6). This was consistent with the fluctuation analysis results shown in Fig. 1B. Furthermore, we observed that the OFX MIC conferred by a given *gyrA* mutation varied depending on the strain it was present in (Fig. 4B; See SI Appendix, Table S6). For example, mutants in the N0157 strain generally had higher OFX MICs than mutants in either the N0145 or N1283 strains. The only mutation that deviated from this trend was GyrA G88C, which conferred a higher OFX MIC when in the N0145 strain. Notably, the GyrA A90V mutation conferred a resistance level equal to or greater than 4 µg/mL OFX in the N0157 and N1283 strains, but not in N0145. This was consistent with the presence of GyrA A90V in the OFX-R mutational profile for N0157 and N1283, but not in N0145, in the

fluctuation analysis using 4 µg/mL OFX (Fig. 1A**;** Fig. 3). In summary, the differences in OFX MIC reflected the strain-dependent mutational profiles for OFX-R in *Mtb*, as expected.

Fitness of ofloxacin-resistance mutations are associated with their relative frequency *in vitro*

While the OFX MICs may determine which mutations may be observed in a fluctuation analysis, it is not the sole parameter to influence the OFX-R mutational profile for a given strain. We found that while the same *gyrA* mutation can be observed in two different *Mtb* strains, their relative frequencies may vary (Fig. 3). This variation may be due to the fitness of a given *gyrA* mutant being different across genetic backgrounds. To test this hypothesis, we used cell growth assays in antibiotic-free conditions to measure the *in vitro* fitness of our panel of OFX-R mutants relative to their respective parental wild-type ancestors. We observed that the relative fitness of the OFX-R mutants was modulated by both the *gyrA* mutation and the *Mtb* strain they were present in (Fig. 5A; See SI Appendix, Fig. S2-S3, Table S7). Furthermore, there was a positive association between the fitness of a given *gyrA* mutation with its relative frequency in the fluctuation analysis for the N0157 and N1283 strains (Fig. 5B, $P = 0.03$ for N0157, $P = 0.05$ for N1283). There was no evidence of an association in the N0145 background due to the lack of GyrA G88C and A90V mutants in its fluctuation analysis.

The results from Fig. 4 and Fig. 5, as well as the apparent lack of mutation rate differences between our strains (Fig. 1C), suggested that differential mutational profiles was an important contributor in the variation in OFX-R frequency in *Mtb*. These mutational profile differences appear to be driven by the *Mtb* genetic background's effect on both the MIC and the relative fitness cost of OFX-R mutations. We next explored whether these *in vitro* results would be relevant in clinical settings.

230

231 **Mutational profile for fluoroquinolone-resistance *in vitro* reflects clinical observations**

232 To explore the clinical relevance of our *in vitro* work, we surveyed the FQ-R mutational
233 profile from publicly available *Mtb* genomes obtained from clinical isolates. FQs are generally
234 used for treatment against MDR-TB (29). While it is unclear whether resistance mutations for
235 isoniazid (INH) and/or rifampicin (RIF) predispose a strain to become FQ-R, the prevalence of
236 FQ-R is heavily biased towards MDR-TB strains due to treatment practices. We therefore based
237 our analyses on a collated dataset of 3,452 publicly available MDR-TB genomes (See SI
238 Appendix, Table S8), which we confirmed to be MDR-TB based on the presence of known INH-
239 and RIF-resistance mutations. This dataset provided a reasonable sampling of the overall genetic
240 diversity of *Mtb*, as six of the seven known phylogenetic *Mtb* lineages were represented
241 (Lineages 1 – 6) (17, 30). We catalogued their FQ-R mutational profiles, and found 950 FQ-R
242 mutations in 854 genomes (See SI Appendix, Tables S9-S10), showing that multiple FQ-R
243 mutations may be present in the genome of a single *Mtb* clinical isolate. The frequency of FQ-R
244 differed between lineages, with the highest frequencies present in L2 and L4 strains ($P < 2.2 \times$
245 10^{-16}, Chi-square Goodness of Fit Test). Moreover, we noticed a lineage-dependent mutational
246 profile for FQ-R (Fig. 6, $P = 3.00 \times 10^{-5}$, Fisher's exact test; See SI Appendix, Fig. S4, Tables
247 S10-S11). For example, while the GyrA D94G mutation was most prevalent in strains belonging
248 to L1, L2, and Lineage 3 (L3), the GyrA A90V mutation was most prevalent in L4 and Lineage 6
249 (L6).

250 We observed that the mutational profile for FQ-R in the fluctuation analysis experiments
251 mimicked published clinical data. Firstly, *gyrA* mutations made up the large majority of FQ-R
252 mutations *in vitro* (Fig. 3; See SI Appendix, Tables S4-S5) and 944 out of the 950 QRDR

mutations in the clinic (99.6%; Fig. 6; See SI Appendix, Table S10). The relative frequencies of *gyrA* mutations for each genetic background *in vitro* were also similar to their relative frequencies in the clinic. We compared the frequency of *gyrA* mutations from the OFX-R mutational profile assay in Fig. 3 to our genomic data survey in Fig. 6, but limited it to L2 and L4 strains (the two lineages with the highest clinical frequencies of FQ-R). We observed a positive association between the frequency of a given *gyrA* mutation in our fluctuation analysis compared to the frequency in the clinic, with the association being significant for L2 strains (Fig. 7, P = 0.027 for L2, P = 0.130 for L4, Fisher's exact test). Based on the adjusted R^2 values, 45% of the variability in the clinical frequency of *gyrA* mutations in L2 strains and 19% of the variability in L4 strains can be attributed to how FQ-R evolves in *Mtb in vitro*. As the *in vitro* evolution of FQ-R is itself modulated by the *Mtb* genetic background, this provided evidence for the *Mtb* genetic background's role in the evolution of FQ-R in the clinic.

Discussion

Overall, we illustrate the *Mtb* genetic background's considerable role in the evolution of resistance to FQs, a clinically important antimicrobial. We first explored whether the genetic variation among natural populations of *Mtb* can influence FQ-R evolution *in vitro*. Specifically, considering that *Mtb* treatment regimens are based on standardized antimicrobial concentrations (29), we tested whether different genetic variants of *Mtb* would acquire FQ-R at the same frequency when exposed to the same concentration of FQ. Fluctuation analysis on nine, genetically distinct, drug-susceptible *Mtb* strains showed that the genetic background can have a drastic effect on the rate of OFX-R acquisition when using the same concentration of OFX (Fig. 1). However, the effect of the genetic background on AMR frequencies observed here in the

context of OFX-R differed from those reported in previous work focusing on other antibiotics. Specifically, experimental evidence from Ford *et al.* suggested that L2 Beijing strains have a higher basal DNA mutation rate compared to L4 (11), which consequently leads to a higher frequency of resistance against INH, RIF and ethambutol, even after correcting for differences in AMR mutational profiles. Based on these results, one would expect that L2 Beijing strains would also show higher frequencies of FQ-R. However, this was not the case in our fluctuation analysis for OFX-R, as one of our L2 Beijing strains (N0145) repeatedly acquired the lowest frequency of OFX-R (Fig. 1). Moreover, we saw minimal, if any, DNA base-pair mutation rate differences between three *Mtb* strains with different *in vitro* OFX-R frequencies (Fig. 2). Contradicting results on the *in vitro* frequency of AMR in *Mtb* have been reported before, with other fluctuation analyses showing no difference in the frequency of RIF-R emergence between L2 Beijing and non-L2 Beijing strains (52). Although diverging in their results, these previous studies, together with the study conducted here, highlight the importance of the genetic background when testing for the frequency of AMR in *Mtb*. Furthermore, these results show that differential DNA mutation rate is not the only parameter relevant in determining the frequency of FQ-R in *Mtb*.

If DNA mutation rates do not contribute to the variation in OFX-R frequency, we hypothesized that differences in the phenotypic effects of OFX-R mutations, and their consequent effect on the mutational profiles for OFX-R, may be important contributors. By sequencing the QRDR from resistant colonies in our OFX fluctuation analysis, we observed strain-specific patterns in the mutational profiles for OFX-R (Fig. 3). This suggested that the mutational profile for FQ-R is not only a function of the FQ type and concentration (10, 14, 47, 53), but that epistatic interactions between a given FQ-R mutation and the genetic background may also play a role. Similar epistatic interactions have been observed in *Escherichia coli* (26), *Pseudomonas*

299 spp. (16, 27), *M. smegmatis* (54), and *Mtb* (24, 28, 31), where a given RIF-R *rpoB* mutation
300 conferred differential MIC and fitness costs depending on the genetic background it occurred in,
301 or on the presence of other AMR mutations. In line with these previous studies, we found that the
302 OFX MIC and the fitness effect conferred by a given *gyrA* mutation varied significantly
303 depending on the *Mtb* genetic background they occur in (Fig. 4; Fig. 5A; See SI Appendix, Table
304 S6). These results support the hypothesis that epistasis plays a role in determining the strain-
305 dependent OFX-R frequencies and mutational profiles observed during our fluctuation analyses
306 (Fig. 3; Fig. 5B).

307 These epistatic interactions may have clinical consequences. A recent study has shown
308 that drug-susceptible *Mtb* strains with higher MICs to INH and RIF were associated with
309 increased risk of relapse following first-line treatment (20). Specific FQ-R *gyrA* mutations have
310 also been associated with poorer treatment outcomes in MDR-TB patients (40, 55). Considering
311 our observation that the *Mtb* genetic background affected both the OFX MICs and OFX-R
312 mutational profiles (Fig. 3; Fig. 4; See SI Appendix, Tables S4-S6), the genetic background may
313 therefore contribute to differences in patient treatment outcomes when using FQs as first-line
314 drugs.

315 Using publicly available genomic data from *Mtb* clinical isolates, we observed significant
316 lineage-dependent variation in the frequency of and mutational profiles for FQ-R (Fig. 6). As
317 expected, the vast majority of FQ-R mutations were observed in *gyrA* (10, 22, 38, 39, 41–43).
318 FQ-R was also most frequent in L2 and L4. This was also as expected, as strains from the L2
319 Beijing sublineage are known to associate with MDR-TB (4, 15, 21, 22), while L4 strains are the
320 most prevalent globally, including in regions classified as high-burden for TB (17, 29, 56, 57).
321 Consequently, strains from L2 and L4 would be more exposed to FQs, leading to the higher FQ-

R frequencies observed in these two lineages. Furthermore, we observed that almost half of the variability in the clinical frequency of *gyrA* mutations of L2 strains can be explained by how *Mtb* evolves *in vitro* (Fig. 7). However, the *in vitro* FQ-R evolution could only account for 19% of the variability for *gyrA* mutation frequencies in clinical L4 strains. This suggested that while the *Mtb* genetic background can influence the evolution of FQ-R in the clinic, other factors (which may be independent of the *Mtb* genetic background) likely played strong roles as well. Epidemiological factors including socioeconomic disruptions, health system inefficiencies, and human behaviour are well known risk factors for the emergence and transmission of AMR in *Mtb* (3–7). Meanwhile, biological factors not explored in this study, such as antibiotic type and concentration (10–13, 46, 47), pharmacodynamic and pharmacokinetic features (58, 59), and the selective pressure of the host immune system (60), may also influence the evolution of FQ-R.

Our study is limited by the fact that our survey of clinical FQ-R frequencies involved a genomic dataset that was sampled by convenience. This dataset was used due to its public availability, and may not be fully representative of FQ-R frequencies in *Mtb* populations. We noted that lineage-specific frequencies of FQ-R were likely biased due to the overrepresentation L2 and L4 strains. Thus, to acquire a better understanding on which FQ-R mutations appeared and at what frequency they occurred at in different *Mtb* lineages, either more genomes from clinical isolates from other *Mtb* lineages must be made available, or a population-based study must be undertaken, preferably in a high burden MDR-TB region.

Exposure to quinolones have been shown to lead to SOS response-mediated mutagenesis, which can increase the rate of AMR acquisition, including resistance to quinolones themselves (53, 61, 62). Therefore, the strain-dependent OFX-R acquisition rates (Fig. 1) may be due to strain-dependent differences in the magnitude of quinolone-induced mutagenesis. We did not

345 explicitly test for this possibility. However, phylogenetic SNPs present in SOS response-related
346 genes may lead to strain-dependent differences in quinolone-induced mutagenesis, and we
347 observed no such SNPs present across our panel of drug-susceptible *Mtb* strains (See SI
348 Appendix, Table S2) (49). Thus, we observed no genetic evidence for strain-specific SOS
349 response-mediated mutagenesis. Furthermore, in *E. coli*, quinolone-induced quinolone-resistant
350 mutations may only be observed after 5 days of incubation with quinolones, which is equivalent
351 to approximately 225 generations for wild-type *E. coli* (53, 61). Meanwhile, our wild-type *Mtb*
352 strains were incubated for 40 generations at most in the presence of OFX (see Materials and
353 Methods; See SI Appendix, Table S7), making the likelihood of observing OFX-induced OFX-R
354 mutants in our *in vitro* system extremely low.

355 Another limitation of our study is that fluctuation analyses only model AMR emergence.
356 Long-term population dynamics also play an important role in AMR evolution (8, 12, 14). For
357 example, population bottleneck events modulate AMR evolution during serial transfer
358 experiments (14, 27, 63, 64), and have also been hypothesized to strongly influence *Mtb*
359 evolution in the clinic (65). Thus, modeling FQ-R evolution in *Mtb* in epidemiological settings
360 would benefit from the use of some measure of long-term population dynamics and between-host
361 transmission. Nevertheless, the fitness of AMR mutants is an important factor in determining its
362 evolutionary fate (8, 9, 12, 14, 26, 54, 64) and its potential for between-host transmission (63, 66,
363 67). Considering that the *Mtb* genetic background modulated the fitness effect of FQ-R mutations
364 (Fig. 5; See SI Appendix, Table S7), the genetic background may modulate how likely FQ-R
365 mutants transmit between patients.

366 In conclusion, we illustrate how the genetic variation present in natural populations of
367 *Mtb* modulates FQ-R evolution. Considering the non-random geographic distribution of different

368 *Mtb* genetic variants (17, 30), our work suggests that there may be regional differences in the rate
369 of FQ-R emergence and FQ-R prevalence when using FQs as a first-line drug. We therefore
370 highlight the importance of bacterial genetics in determining how FQ-R evolves in *Mtb* and, in
371 general, how AMR evolves in pathogens.
372
373

Materials and Methods

Collection of drug-susceptible clinical isolates of *M. tuberculosis* strains for *in vitro* studies

We used nine genetically-distinct *Mtb* strains, with three strains from each of the following *Mtb* lineages: Lineage 1 (L1; also known as the East-Africa and India Lineage), Lineage 2 (L2; the East Asian Lineage), and Lineage 4 (L4; the Euro-American Lineage) (17, 68). All strains were previously isolated from patients, fully drug-susceptible, and previously characterized by Borrell *et al*. (49) (See SI Appendix, Table S1).

Prior to all experimentation, starter cultures for each *Mtb* strain were prepared by recovering a 20 μL aliquot from frozen stocks into a 10 mL volume of Middlebrook 7H9 broth (BD), supplemented with an albumin (Fraction V, Roche), dextrose (Sigma-Aldrich), catalase (Sigma-Aldrich), and 0.05% Tween® 80 (AppliChem) (hereafter designated as 7H9 ADC). These starter cultures were incubated until their optical density at wavelength of 600 nm (OD_{600}) was approximately 0.50, and were then used for *in vitro* assays.

Fluctuation analyses

Fluctuation analyses were performed as described by Luria & Delbrück (48). Briefly, an aliquot from the starter cultures for each strain was used to inoculate 350 mL of 7H9 ADC to have an initial bacterial density of 5,000 colony forming units (CFU) per mL. This was immediately divided into 33 parallel cultures, each with 10 mL of culture volume aliquoted into individual 50 mL Falcon™ Conical Centrifuge Tubes (Corning Inc.). The parallel cultures were incubated at 37ºC on standing racks, with re-suspension by vortexing (Bio Vortex V1, Biosan) every 24 hours. Cultures were grown until an OD_{600} of between 0.40 to 0.65. Once at this density, final cell counts (N_t) from three randomly chosen parallel cultures were calculated by serial

dilution and plating on Middlebrook 7H11 (BD), supplemented with oleic acid (AppliChem), albumin, and catalase (hereafter referred to as 7H11 OADC). To calculate the number of resistant colonies (*r*), the remaining 30 parallel cultures not used for N_t determination were pelleted at 800 g for 10 min. at 4ºC using the Allegra X-15R Benchtop Centrifuge (Beckmann Coulter). The supernatants were discarded, and the bacterial pellets re-suspended in 300 µL of 7H9 ADC. The re-suspensions were spread on 7H11 OADC plates supplemented with the relevant drug concentration (2, 4, or 8 µg/mL of ofloxacin, or 100 µg/mL streptomycin; Sigma). Resistant colonies were observed and enumerated after 21 to 35 days of incubation, depending on the *Mtb* strain. The estimated number of mutations per culture (*m*) was estimated from the distribution of frequency of drug-resistance per cell (r_{dist}) using the Ma, Sarkar, Sandri-Maximum Likelihood Estimator method (MSS-MLE) (69). The frequency of drug-resistance acquired per cell (*F*) per strain was then calculated by dividing the calculated *m* values by their respective N_t values. The 95% confidence intervals for each *F* were calculated as previously described by Rosche & Foster (69). Hypotheses testing for significant differences between the r_{dist} between strains for the fluctuation analyses at 4 µg/mL of OFX (Fig. 1A) and at 100 µg/mL of STR (Fig. 1C) were performed using the Kruskal-Wallis test; significant differences in the r_{dist} between strains in the fluctuation analyses at 2 and 8 µg/mL (Fig. 1B) were tested for using the Wilcoxon rank-sum test. Statistical analyses were performed using the R statistical software (70).

Determining the mutational profile for ofloxacin-resistance *in vitro*

From the parallel cultures plated on 4 µg/mL of OFX (Fig. 1A), up to 120 resistant colonies per strain (at least 1 colony per plated parallel culture if colonies were present, to a maximum of 6) were transferred into 100 µL of sterile deionized H_2O placed in Falcon® 96-well

420 Clear Microplate (Corning Inc.). The bacterial suspensions were then heat-inactivated at 95ºC for
421 1 h, and used as PCR templates to amplify the QRDR in *gyrA* and *gyrB* using primers designed
422 by Feuerriegel *et al.* (71). PCR products were sent to Macrogen, Inc. or Microsynth AG for
423 Sanger sequencing, and QRDR mutations were determined by aligning the PCR product
424 sequences against the H37Rv reference sequence (72). Sequence alignments were performed
425 using the Staden Package, while the amino acid substitutions identification were performed using
426 the Molecular Evolutionary Genetics Analysis Version 6.0 package. Fisher's exact test was used
427 to test for significant differences between the strains' mutational profiles for OFX-R. Data
428 analyses were performed using the R statistical software (70).
429
430 **Isolation of spontaneous ofloxacin-resistant mutants**
431 Spontaneous OFX-resistant mutants were isolated from strains belonging one of three
432 genetic backgrounds: N0157 (L1, Manila sublineage; high frequency of OFX-R), N1283 (L4,
433 Ural sublineage; mid-frequency of OFX-R), and N0145 (L2, Beijing sublineage; low frequency
434 of OFX-R). To begin, we transferred 50 µL of starter cultures for each strain into separate culture
435 tubes containing 10 mL of fresh 7H9 ADC. Cultures were incubated at 37ºC until OD_{600} of
436 approximately 0.80, and pelleted at 800 *g* for 5 min at 4ºC. The supernatant was discarded, and
437 the pellet re-suspended in 300 µL of 7H9 ADC. The re-suspension was plated on 7H11 OADC
438 (BD) supplemented with 2 µg/mL of OFX, and incubated until resistant colonies appeared
439 (approximately 14 to 21 days). Resistant colonies were picked and re-suspended in fresh 10 mL
440 7H9 ADC, and incubated at 37ºC. Once the culture reached early stationary phase, two aliquots
441 were prepared. The first aliquot was heat-inactivated at 95ºC for 1 h, and the *gyrA* mutation
442 identified by PCR and Sanger sequencing, as described in the mutational profile for OFX-R

443 assay. If the first aliquot harboured one of four OFX-r *gyrA* mutations ($GyrA^{D94G}$, $GyrA^{D94N}$,
444 $GyrA^{A90V}$, or $GyrA^{G88C}$), the second aliquot was stored in -80ºC for future use.

445 Prior to further experimentation with the spontaneously OFX-R mutant strains, starter
446 cultures were prepared in the same manner as for the drug-susceptible strains.

447

448 **Drug susceptibility assay**

449 We determined the OFX-susceptibility levels of our spontaneous OFX-resistant mutants
450 and their respective drug-susceptible ancestors by performing the colorimetric, microtiter plate-
451 based Alamar Blue assay (73). Briefly, we used a Falcon® 96-well Clear Microplate, featuring a
452 serial two-fold dilution of OFX. For drug-susceptible strains, a range of OFX concentration from
453 15 µg/mL to 0.058 µg/mL was used. Meanwhile, for OFX-resistant strains, a range of 60 µg/mL
454 to 0.234 µg/mL was used. Each well was inoculated with a 10 µL volume of starter culture to
455 have a final inoculum of approximately 5×10^6 CFU/mL. The plates were incubated at 37ºC for
456 10 days. Following incubation, 10 µL of Resazurin (Sigma) was added to each well, and the
457 plates were incubated for another 24 h at 37ºC. After this incubation period, plates were
458 inactivated by adding 100 µL of 4% formaldehyde to every well. Measurement of fluorescence
459 produced by viable cells was performed on SpectraMAX GeminiXPS Microplate Reader
460 (Molecular Devices). The excitation wavelength was set at 536 nm, and the emission wavelength
461 at 588 nm was measured. Minimum inhibitory concentration (MIC) for OFX was determined by
462 first fitting a Hill curve to the distribution of fluorescence, and then defining the MIC as the
463 lowest OFX concentration where the fitted Hill curve showed a ≥95% reduction in fluorescence.
464 Two sets of experiments were performed for every strain, with three technical replicates per

465 experiment. Analyses of MIC data were performed and figures created using the numpy, scipy,
466 pandas and matplotlib modules for the Python programming language.
467
468 **Cell growth assay**
469 We set up three or four 1,000 mL roller bottles with 90 mL of 7H9 ADC and 10 mL
470 borosilicate beads. Each bottle was inoculated with a volume of starter cultures so that the initial
471 bacterial density was at an OD_{600} of 5×10^{-7}. The inoculated bottles were then placed in a roller
472 incubator set to 37ºC, and incubated for 12 to 18 days with continuous rolling. OD_{600}
473 measurements were taken once or twice every 24 hours. Two independent experiments in either
474 triplicates or quadruplicates were performed per strain.
475 We defined the exponential phase as the bacterial growth phase where we observed a
476 $\log_2$-linear relationship between OD_{600} and time; specifically, we used a Pearson's R^2 value $\geq$
477 0.98 as the threshold. The growth rate of a particular strain was then defined as the slope of the
478 linear regression model. The relative fitness of a given spontaneous OFX-R mutant was defined
479 by taking the growth rate of the OFX-resistant mutant strain and dividing it by the growth rate of
480 its respective drug-susceptible ancestor. Linear regression models for the cell growth assays data
481 were performed using the numpy, scipy, pandas and matplotlib modules for the Python
482 programming language, as well as the R statistical software (70).
483
484 **Surveying the fluoroquinolone-resistance profile from publicly available *M. tuberculosis***
485 **genomes**
486 We screened public databases to download global representatives of *Mtb* genomes, as
487 described by Menardo *et al*. (74). We selected genomes that were classified as MDR-TB based

488 on the presence of both isoniazid (INH)- and rifampicin (RIF)-resistance mutations. This
489 provided a dataset of 3,452 genomes with confirmed MDR-TB; their accession numbers are
490 reported in Table S8 (See SI Appendix). These MDR-TB genomes were then screened for the
491 presence of FQ-resistance mutations, and we identified 854 genomes that were classified as FQ-
492 R.

493 The INH-, RIF-, and FQ-resistance mutations used for screening are the same mutations
494 used by Payne, Menardo *et al*. (75), and are listed in Table S12 (See SI Appendix). A drug-
495 resistance mutation was defined as "fixed" in the population when it reached a frequency of
496 ≥90%. Meanwhile, a drug-resistance mutation was considered "variable" in the population when
497 its frequency was between 10% to 90%; thus, multiple drug-resistance mutations may be present
498 in the genomic data from a single *Mtb* clinical isolate.

499

500 **Acknowledgements**

501 The authors would like to thank Sebastian Bonhoeffer, Daniel Angst, and Diarmaid Hughes for
502 providing critical comments on the manuscript. Calculations were performed at sciCORE
503 (http://scicore.unibas.ch/) scientific computing core facility at University of Basel. Library
504 preparation and sequencing was carried out in the Genomics Facility Basel. This work was
505 supported by the Swiss National Science Foundation (grants 310030_166687, IZRJZ3_164171,
506 IZLSZ3_170834 and CRSII5_177163), the European Research Council (309540-EVODRTB)
507 and SystemsX.ch.

508

509 **References**

510 1. MacGowan AP (2008) Clinical implications of antimicrobial resistance for therapy. *J*
511 *Antimicrob Chemother* 62(Suppl_2):ii105-ii114.
512 2. Winston CA, Mitruka K (2002) Treatment duration for patients with drug-resistant
513 tuberculosis, United States. *Emerg Infect Dis* 18(7):1201–1202.
514 3. Dalton T, et al. (2012) Prevalence of and risk factors for resistance to second-line drugs in
515 people with multidrug-resistant tuberculosis in eight countries: a prospective cohort study. *The*
516 *Lancet* 380(9851):1406–1417.
517 4. Merker M, et al. (2015) Evolutionary history and global spread of the *Mycobacterium*
518 *tuberculosis* Beijing lineage. *Nat Genet* 47(3):242–249.
519 5. Alvarez-Uria G, Gandra S, Laxminarayan R (2016) Poverty and prevalence of
520 antimicrobial resistance in invasive isolates. *Int J Infect Dis* 52:59–61.
521 6. Eldholm V, et al. (2016) Armed conflict and population displacement as drivers of the
522 evolution and dispersal of *Mycobacterium tuberculosis*. *Proc Natl Acad Sci* 113(48):13881–
523 13886.
524 7. Shah NS, et al. (2017) Transmission of Extensively Drug-Resistant Tuberculosis in South
525 Africa. *N Engl J Med* 376(3):243–253.
526 8. zur Wiesch PA, Kouyos R, Engelstädter J, Regoes RR, Bonhoeffer S (2011) Population
527 biological principles of drug-resistance evolution in infectious diseases. *Lancet Infect Dis*
528 11(3):236–247.
529 9. Hughes D, Andersson DI (2017) Evolutionary Trajectories to Antibiotic Resistance. *Annu*
530 *Rev Microbiol* 71(1):579–596.
531 10. Zhou J, et al. (2000) Selection of Antibiotic-Resistant Bacterial Mutants: Allelic Diversity
532 among Fluoroquinolone-Resistant Mutations. *J Infect Dis* 182(2):517–525.

533 11. Ford CB, et al. (2013) *Mycobacterium tuberculosis* mutation rate estimates from different
534 lineages predict substantial differences in the emergence of drug-resistant tuberculosis. *Nat Genet*
535 45(7):784–790.
536 12. Lindsey HA, Gallie J, Taylor S, Kerr B (2013) Evolutionary rescue from extinction is
537 contingent on a lower rate of environmental change. *Nature* 494(7438):463–467.
538 13. McGrath M, Gey van Pittius NC, van Helden PD, Warren RM, Warner DF (2014)
539 Mutation rate and the emergence of drug resistance in *Mycobacterium tuberculosis*. *J Antimicrob*
540 *Chemother* 69(2):292–302.
541 14. Huseby DL, et al. (2017) Mutation Supply and Relative Fitness Shape the Genotypes of
542 Ciprofloxacin-Resistant *Escherichia coli*. *Mol Biol Evol* 34(5):1029–1039.
543 15. Fenner L, et al. (2012) Effect of Mutation and Genetic Background on Drug Resistance in
544 *Mycobacterium tuberculosis*. *Antimicrob Agents Chemother* 56(6):3047–3053.
545 16. Vogwill T, Kojadinovic M, Furió V, MacLean RC (2014) Testing the Role of Genetic
546 Background in Parallel Evolution Using the Comparative Experimental Evolution of Antibiotic
547 Resistance. *Mol Biol Evol* 31(12):3314–3323.
548 17. Gagneux S (2018) Ecology and evolution of *Mycobacterium tuberculosis*. *Nat Rev*
549 *Microbiol* 16(4):202–213.
550 18. Ängeby KA, et al. (2010) Wild-type MIC distributions of four fluoroquinolones active
551 against *Mycobacterium tuberculosis* in relation to current critical concentrations and available
552 pharmacokinetic and pharmacodynamic data. *J Antimicrob Chemother* 65(5):946–952.
553 19. Coeck N, et al. (2016) Correlation of different phenotypic drug susceptibility testing
554 methods for four fluoroquinolones in *Mycobacterium tuberculosis*. *J Antimicrob Chemother*
555 71(5):1233–1240.

556 20. Colangeli R, et al. (2018) Bacterial Factors That Predict Relapse after Tuberculosis
557 Therapy. *N Engl J Med* 379(9):823–833.
558 21. Borrell S, Gagneux S (2009) Infectiousness, reproductive fitness and evolution of drug-
559 resistant *Mycobacterium tuberculosis*. *Int J Tuberc Lung Dis Off J Int Union Tuberc Lung Dis*
560 13(12):1456–1466.
561 22. Wollenberg KR, et al. (2017) Whole-Genome Sequencing of *Mycobacterium tuberculosis*
562 Provides Insight into the Evolution and Genetic Composition of Drug-Resistant Tuberculosis in
563 Belarus. *J Clin Microbiol* 55(2):457–469.
564 23. Oppong YEA, et al. (2019) Genome-wide analysis of Mycobacterium tuberculosis
565 polymorphisms reveals lineage-specific associations with drug resistance. *BMC Genomics*
566 20(1):252.
567 24. Gagneux S, et al. (2006) The Competitive Cost of Antibiotic Resistance in
568 *Mycobacterium tuberculosis*. *Science* 312(5782):1944–1946.
569 25. Decuypere S, et al. (2012) Molecular Mechanisms of Drug Resistance in Natural
570 Leishmania Populations Vary with Genetic Background. *PLoS Negl Trop Dis* 6(2):e1514.
571 26. Angst DC, Hall AR (2013) The cost of antibiotic resistance depends on evolutionary
572 history in *Escherichia coli*. *BMC Evol Biol* 13(1):163.
573 27. Vogwill T., Kojadinovic M., MacLean R. C. (2016) Epistasis between antibiotic
574 resistance mutations and genetic background shape the fitness effect of resistance across species
575 of *Pseudomonas*. *Proc R Soc B Biol Sci* 283(1830):20160151.
576 28. Trauner A, et al. (2018) Resource misallocation as a mediator of fitness costs in antibiotic
577 resistance. *bioRxiv*:456434.

578 29. World Health Organization (2017) *Global tuberculosis report 2018* (Geneva,
579 Switzerland) Available at: https://www.who.int/tb/publications/global_report/en/.
580 30. Comas I, et al. (2010) Human T cell epitopes of *Mycobacterium tuberculosis* are
581 evolutionarily hyperconserved. *Nat Genet* 42(6):498–503.
582 31. Zaczek A, Brzostek A, Augustynowicz-Kopec E, Zwolska Z, Dziadek J (2009) Genetic
583 evaluation of relationship between mutations in *rpoB* and resistance of *Mycobacterium*
584 *tuberculosis* to rifampin. *BMC Microbiol* 9(1):10.
585 32. Imperial MZ, et al. (2018) A patient-level pooled analysis of treatment-shortening
586 regimens for drug-susceptible pulmonary tuberculosis. *Nat Med* 24(11):1708–1715.
587 33. Vjecha MJ, Tiberi S, Zumla A (2018) Accelerating the development of therapeutic
588 strategies for drug-resistant tuberculosis. *Nat Rev Drug Discov* 17(5):377.
589 34. Gillespie SH, et al. (2014) Four-Month Moxifloxacin-Based Regimens for Drug-Sensitive
590 Tuberculosis. *N Engl J Med* 371(17):1577–1587.
591 35. Jindani A, et al. (2014) High-Dose Rifapentine with Moxifloxacin for Pulmonary
592 Tuberculosis. *N Engl J Med* 371(17):1599–1608.
593 36. Merle CS, et al. (2014) A Four-Month Gatifloxacin-Containing Regimen for Treating
594 Tuberculosis. *N Engl J Med* 371(17):1588–1598.
595 37. Takiff H, Guerrero E (2011) Current Prospects for the Fluoroquinolones as First-Line
596 Tuberculosis Therapy. *Antimicrob Agents Chemother* 55(12):5421–5429.
597 38. Takiff HE, et al. (1994) Cloning and nucleotide sequence of *Mycobacterium tuberculosis*
598 gyrA and gyrB genes and detection of quinolone resistance mutations. *Antimicrob Agents*
599 *Chemother* 38(4):773–780.

600 39. Maruri F, et al. (2012) A systematic review of gyrase mutations associated with
601 fluoroquinolone-resistant *Mycobacterium tuberculosis* and a proposed gyrase numbering system.
602 *J Antimicrob Chemother* 67(4):819–831.
603 40. Rigouts L, et al. (2016) Specific *gyrA* gene mutations predict poor treatment outcome in
604 MDR-TB. *J Antimicrob Chemother* 71(2):314–323.
605 41. Piton J, et al. (2010) Structural Insights into the Quinolone Resistance Mechanism of
606 *Mycobacterium tuberculosis* DNA Gyrase. *PLOS ONE* 5(8):e12245.
607 42. Aldred KJ, Blower TR, Kerns RJ, Berger JM, Osheroff N (2016) Fluoroquinolone
608 interactions with *Mycobacterium tuberculosis* gyrase: Enhancing drug activity against wild-type
609 and resistant gyrase. *Proc Natl Acad Sci* 113(7):E839–E846.
610 43. Blower TR, Williamson BH, Kerns RJ, Berger JM (2016) Crystal structure and stability
611 of gyrase–fluoroquinolone cleaved complexes from *Mycobacterium tuberculosis*. *Proc Natl Acad*
612 *Sci* 113(7):1706–1713.
613 44. Boritsch EC, et al. (2016) Key experimental evidence of chromosomal DNA transfer
614 among selected tuberculosis-causing mycobacteria. *Proc Natl Acad Sci* 113(35):9876–9881.
615 45. Gygli SM, Borrell S, Trauner A, Gagneux S (2017) Antimicrobial resistance in
616 *Mycobacterium tuberculosis*: mechanistic and evolutionary perspectives. *FEMS Microbiol Rev*
617 41(3):354–373.
618 46. Mustaev A, et al. (2014) Fluoroquinolone-Gyrase-DNA Complexes TWO MODES OF
619 DRUG BINDING. *J Biol Chem* 289(18):12300–12312.
620 47. Malik M, et al. (2016) Suppression of gyrase-mediated resistance by C7 aryl
621 fluoroquinolones. *Nucleic Acids Res* 44(7):3304–3316.

622 48. Luria SE, Delbrück M (1943) Mutations of Bacteria from Virus Sensitivity to Virus
623 Resistance. *Genetics* 28(6):491–511.
624 49. Borrell S, et al. (2019) Reference set of Mycobacterium tuberculosis clinical strains: A
625 tool for research and product development. *PLOS ONE* 14(3):e0214088.
626 50. Rock JM, et al. (2015) DNA replication fidelity in *Mycobacterium tuberculosis* is
627 mediated by an ancestral prokaryotic proofreader. *Nat Genet* 47(6):677–681.
628 51. Baños-Mateos S, et al. (2017) High-fidelity DNA replication in Mycobacterium
629 tuberculosis relies on a trinuclear zinc center. *Nat Commun* 8(1):855.
630 52. Werngren J, Hoffner SE (2003) Drug-Susceptible *Mycobacterium tuberculosis* Beijing
631 Genotype Does Not Develop Mutation-Conferred Resistance to Rifampin at an Elevated Rate. *J*
632 *Clin Microbiol* 41(4):1520–1524.
633 53. Malik M, Hoatam G, Chavda K, Kerns RJ, Drlica K (2010) Novel Approach for
634 Comparing the Abilities of Quinolones To Restrict the Emergence of Resistant Mutants during
635 Quinolone Exposure. *Antimicrob Agents Chemother* 54(1):149–156.
636 54. Borrell S, et al. (2013) Epistasis between antibiotic resistance mutations drives the
637 evolution of extensively drug-resistant tuberculosis. *Evol Med Public Health* 2013(1):65–74.
638 55. Farhat MR, et al. (2017) Fluoroquinolone Resistance Mutation Detection Is Equivalent to
639 Culture-Based Drug Sensitivity Testing for Predicting Multidrug-Resistant Tuberculosis
640 Treatment Outcome: A Retrospective Cohort Study. *Clin Infect Dis* 65(8):1364–1370.
641 56. Stucki D, et al. (2016) *Mycobacterium tuberculosis* lineage 4 comprises globally
642 distributed and geographically restricted sublineages. *Nat Genet* 48(12):1535–1543.
643 57. Brynildsrud OB, et al. (2018) Global expansion of *Mycobacterium tuberculosis* lineage 4
644 shaped by colonial migration and local adaptation. *Sci Adv* 4(10):eaat5869.

645 58. Pienaar E, et al. (2017) Comparing efficacies of moxifloxacin, levofloxacin and
646 gatifloxacin in tuberculosis granulomas using a multi-scale systems pharmacology approach.
647 *PLOS Comput Biol* 13(8):e1005650.
648 59. Sarathy JP, et al. (2018) Extreme Drug Tolerance of *Mycobacterium tuberculosis* in
649 Caseum. *Antimicrob Agents Chemother* 62(2):e02266-17.
650 60. Handel A, Margolis E, Levin BR (2009) Exploring the role of the immune response in
651 preventing antibiotic resistance. *J Theor Biol* 256(4):655–662.
652 61. Cirz RT, et al. (2005) Inhibition of Mutation and Combating the Evolution of Antibiotic
653 Resistance. *PLOS Biol* 3(6):e176.
654 62. Frenoy A, Bonhoeffer S (2018) Death and population dynamics affect mutation rate
655 estimates and evolvability under stress in bacteria. *PLOS Biol* 16(5):e2005056.
656 63. Comas I, et al. (2012) Whole-genome sequencing of rifampicin-resistant *Mycobacterium*
657 *tuberculosis* strains identifies compensatory mutations in RNA polymerase genes. *Nat Genet*
658 44(1):106–110.
659 64. Barrick JE, Lenski RE (2013) Genome dynamics during experimental evolution. *Nat Rev*
660 *Genet* 14(12):827–839.
661 65. Hershberg R, et al. (2008) High Functional Diversity in *Mycobacterium tuberculosis*
662 Driven by Genetic Drift and Human Demography. *PLOS Biol* 6(12):e311.
663 66. de Vos M, et al. (2013) Putative Compensatory Mutations in the rpoC Gene of Rifampin-
664 Resistant Mycobacterium tuberculosis Are Associated with Ongoing Transmission. *Antimicrob*
665 *Agents Chemother* 57(2):827–832.
666 67. Casali N, et al. (2014) Evolution and transmission of drug-resistant tuberculosis in a
667 Russian population. *Nat Genet* 46(3):279–286.

668 68. Gagneux S, et al. (2006) Variable host–pathogen compatibility in *Mycobacterium*
669 *tuberculosis*. *Proc Natl Acad Sci* 103(8):2869–2873.
670 69. Rosche WA, Foster PL (2000) Determining Mutation Rates in Bacterial Populations.
671 *Methods* 20(1):4–17.
672 70. R Core Team (2018) *R: A language and environment for statistical computing*. (R
673 Foundation for Statistical Computing, Vienna, Austria) Available at: https://www.r-project.org/.
674 71. Feuerriegel S, et al. (2009) Sequence Analyses of Just Four Genes To Detect Extensively
675 Drug-Resistant *Mycobacterium tuberculosis* Strains in Multidrug-Resistant Tuberculosis Patients
676 Undergoing Treatment. *Antimicrob Agents Chemother* 53(8):3353–3356.
677 72. Cole ST, et al. (1998) Deciphering the biology of *Mycobacterium tuberculosis* from the
678 complete genome sequence. *Nature* 393(6685):537–544.
679 73. Franzblau SG, et al. (1998) Rapid, Low-Technology MIC Determination with Clinical
680 *Mycobacterium tuberculosis* Isolates by Using the Microplate Alamar Blue Assay. *J Clin*
681 *Microbiol* 36(2):362–366.
682 74. Menardo F, et al. (2018) Treemmer: a tool to reduce large phylogenetic datasets with
683 minimal loss of diversity. *BMC Bioinformatics* 19(1):164.
684 75. Payne JL, et al. (2019) Transition bias influences the evolution of antibiotic resistance in
685 Mycobacterium tuberculosis. *PLOS Biol* 17(5):e3000265.
686

687 **Figure Legends**

688 **Fig. 1**

689 Variation in the frequency of ofloxacin-resistance between genetically distinct, wild-type *M.*
690 *tuberculosis* strains. **A.** Frequency of ofloxacin-resistance at 4 µg/mL ofloxacin (OFX), as

691 measured by fluctuation analysis. Top panel: Coloured points represent the frequency of resistant
692 mutants per cell per parallel culture, with darker points representing multiple cultures with the
693 same frequency. Colours denote the lineage that the *M. tuberculosis* strain belongs to (L1 = pink;
694 L2 = blue; L4 = red). Grey points represent the estimated number of mutations per cell per strain
695 as calculated by MSS-MLE, while black bars denote the respective 95% confidence intervals.
696 Bottom panel: the percentage of parallel cultures lacking OFX-resistant mutants. **B**. Frequency of
697 ofloxacin-resistance at 2 or 8 µg/mL OFX.
698
699 **Fig. 2**
700 Frequency of streptomycin-resistance at 100 µg/mL streptomycin (STR) for wild-type N0157,
701 N1283, and N0145 *M. tuberculosis* strains, as measured by fluctuation analysis assay. Top panel:
702 Coloured points represent the frequency of resistant mutants per cell per parallel culture, with
703 darker points representing multiple cultures with the same frequency. Colours denote the lineage
704 that the *M. tuberculosis* strain belongs to (L1 = pink; L2 = blue; L4 = red). Grey points represent
705 the estimated number of mutations per cell per strain as calculated by MSS-MLE, while black
706 bars denote the respective 95% confidence intervals. Bottom panel: the percentage of parallel
707 cultures lacking STR-resistant mutants. Two biological replicates are presented for each *M.*
708 *tuberculosis* strain, with each replicate identifier suffixed after the strain name.
709
710 **Fig. 3**
711 Variation in the mutational profile for ofloxacin-resistance after fluctuation analyses using nine
712 genetically-distinct *M. tuberculosis* strains. **A.** Mutations in the quinolone-resistance-determining
713 region (QRDR) of *gyrA* was analyzed in 680 ofloxacin (OFX)-resistant colonies from the

714 fluctuation analysis performed in Fig. 2A (nm = no identified QRDR *gyrA* mutations). Strains are
715 ordered left to right based on their frequency of OFX-resistance at 4 µg/mL OFX. Numbers of
716 colonies analyzed per strain are reported directly above each column. **B**. The number of unique
717 QRDR *gyrA* mutations per *M. tuberculosis* strain for OFX-resistance. Bar colours denote the *M.*
718 *tuberculosis* lineage the strain belongs to (L1 = pink; L2 = blue; L4 = red).
719
720 **Fig. 4**
721 Ofloxacin (OFX) MIC is modulated by the genetic background of *M. tuberculosis*. **A.** Heat-map
722 of OFX-susceptibility via Alamar Blue assay for *gyrA* mutant strains of *M. tuberculosis*, as well
723 as their wild-type ancestor, in three genetic backgrounds (N0157, N0145, or N1283). Light areas
724 represent growing cultures, while dark areas represent non-growing cultures. Yellow points
725 represent estimates for OFX MIC (≥95% reduction in fluorescence). Areas of solid black colours
726 (at 16+ µg/ml OFX for wild-type) and solid yellow colours (at <0.125 µg/ml OFX for mutants)
727 were not measured and coloured in for illustrative purposes. **B**. OFX MIC estimates for each
728 strain per genetic background, superimposed. Coloured points and lines represent MIC
729 measurements for highlighted genetic background, with the line colour denoting the lineage that
730 the strain belongs to (L1 = pink, L2 = blue, L4 = red). Grey points and lines represent the other
731 two genetic backgrounds.
732
733 **Fig. 5**
734 The *M. tuberculosis* genetic background modulates the fitness effect of fluoroquinolone-
735 resistance mutations. **A.** Fitness of ofloxacin-resistant *M. tuberculosis* strain with specified *gyrA*
736 mutation relative to the fitness of their respective wild-type ancestral strain. Ancestral strain per

737 *gyrA* mutant is indicated in the grey bar above each panel. Fitness was measured by cell growth
738 assay in antibiotic-free conditions. **B**. Association between the relative fitness of specified *gyrA*
739 mutant and their absolute frequency during the fluctuation analysis performed in Fig. 1A, in three
740 genetic backgrounds (N0157, N1283, and N0145).
741
742 **Fig. 6**
743 Mutational profile for fluoroquinolone-resistance *gyrA* mutations in clinical isolates of *M.*
744 *tuberculosis*, per lineage. An initial dataset consisting of 3,452 genomes with confirmed MDR-
745 TB mutations were surveyed. 854 genomes were identified as fluoroquinolone-resistant, with 848
746 of these genomes containing *gyrA* mutations. Only fixed fluoroquinolone-resistance mutations in
747 the *gyrA* gene are enumerated here (n = 710). No fixed mutations were observed in L5 strains.
748 Numbers of genomes analyzed per lineage are presented directly below their respective bar
749 graph.
750
751 **Fig. 7**
752 Association between the clinical frequencies of fluoroquinolone-resistance *gyrA* mutations with
753 their respective *in vitro* frequencies amongst *M. tuberculosis* strains belonging to either the L2 or
754 L4 lineages. Clinical frequencies are identical as reported in Fig. 6, while the *in vitro* frequencies
755 are the same as in Fig. 3A, grouped by lineage.

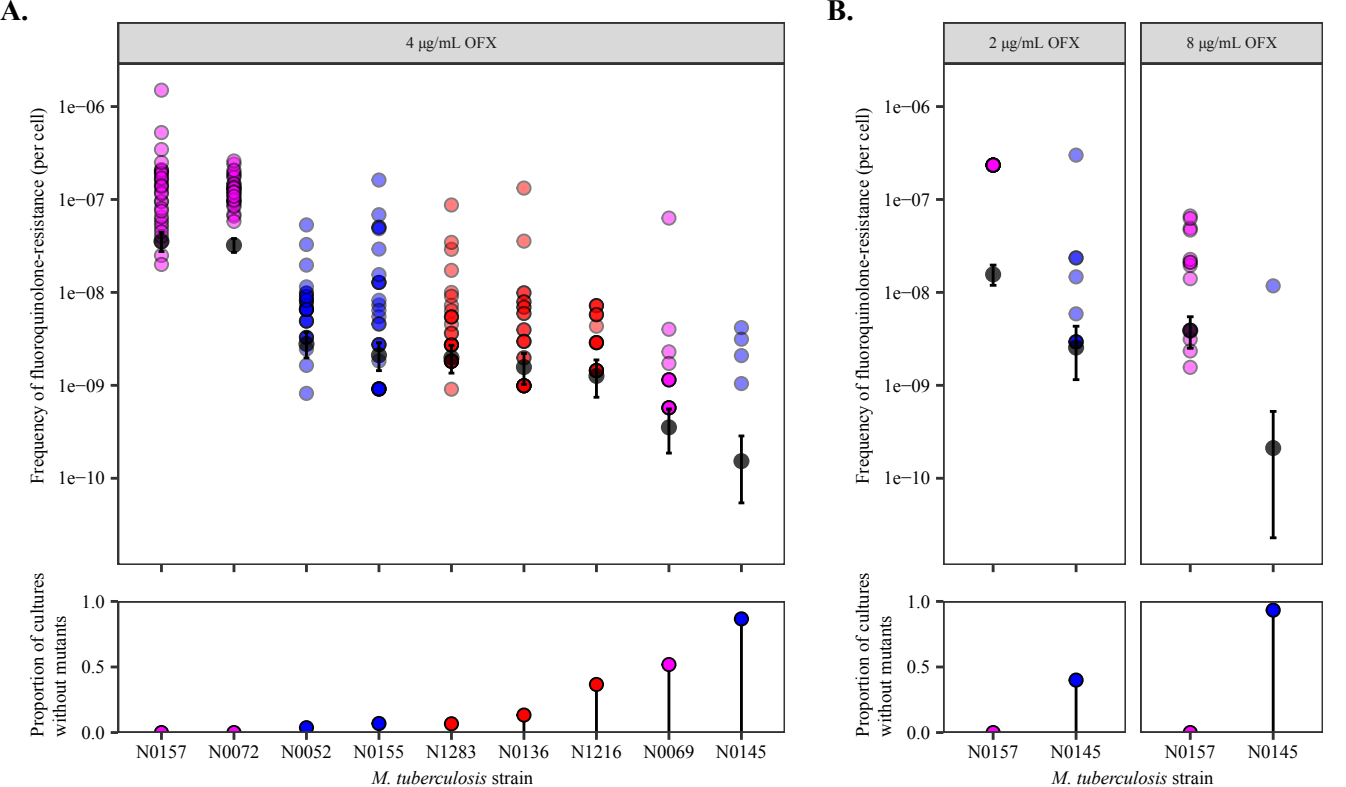
A.
4 µg/mL OFX
Frequency of fluoroquinolone-resistance (per cell)
1e−06
1e−07
1e−08
1e−09
1e−10
Proportion of cultures without mutants
1.0
0.5
0.0
N0157
N0072
N0052
N0155
N1283
N0136
N1216
N0069
N0145
M. tuberculosis strain
B.
2 µg/mL OFX
8 µg/mL OFX
Frequency of fluoroquinolone-resistance (per cell)
1e−06
1e−07
1e−08
1e−09
1e−10
Proportion of cultures without mutants
1.0
0.5
0.0
N0157
N0145
N0157
N0145
M. tuberculosis strain

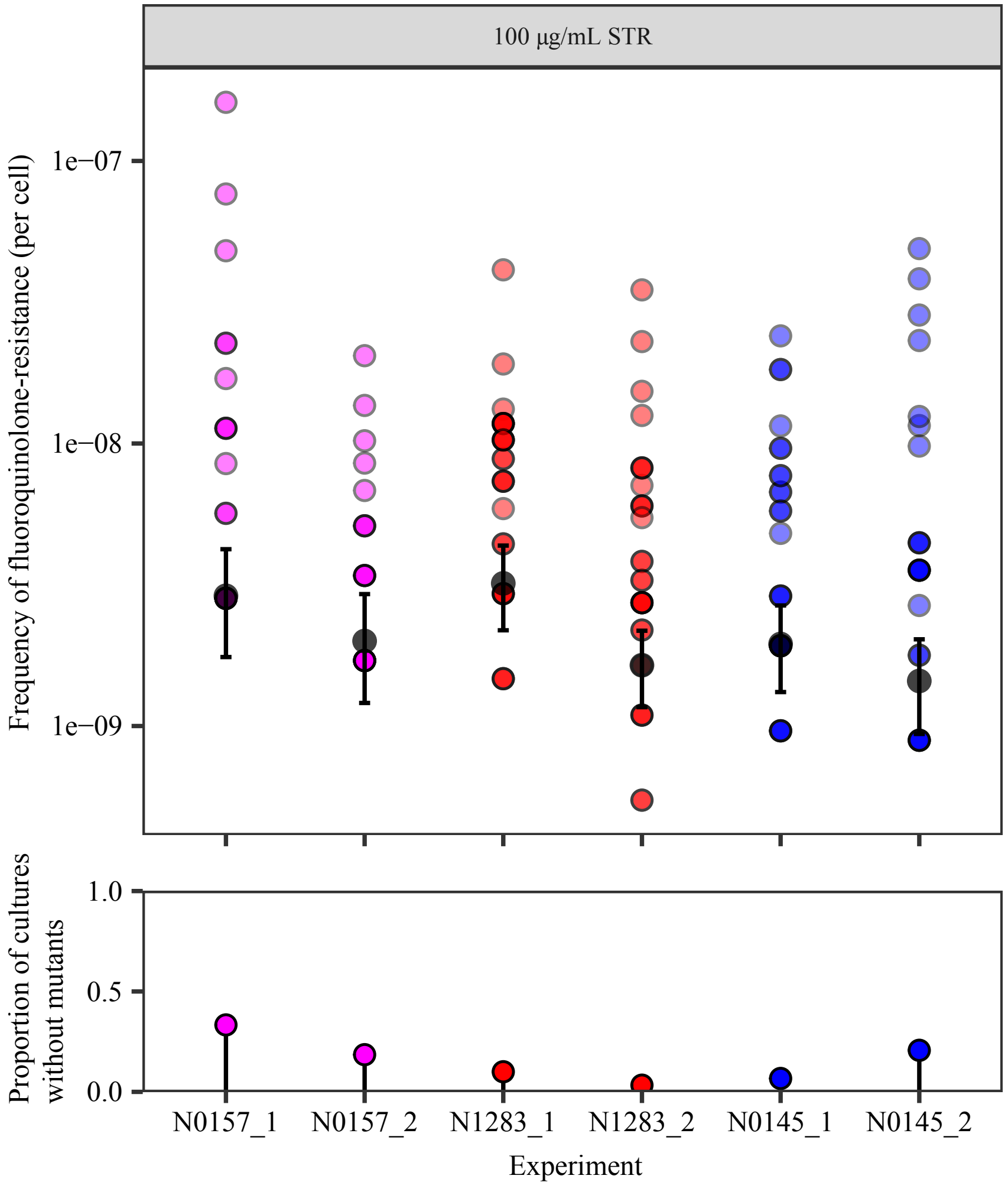
100 µg/mL STR
Frequency of fluoroquinolone-resistance (per cell)
1e−07
1e−08
1e−09
Proportion of cultures without mutants
1.0
0.5
0.0
N0157_1
N0157_2
N1283_1
N1283_2
N0145_1
N0145_2
Experiment

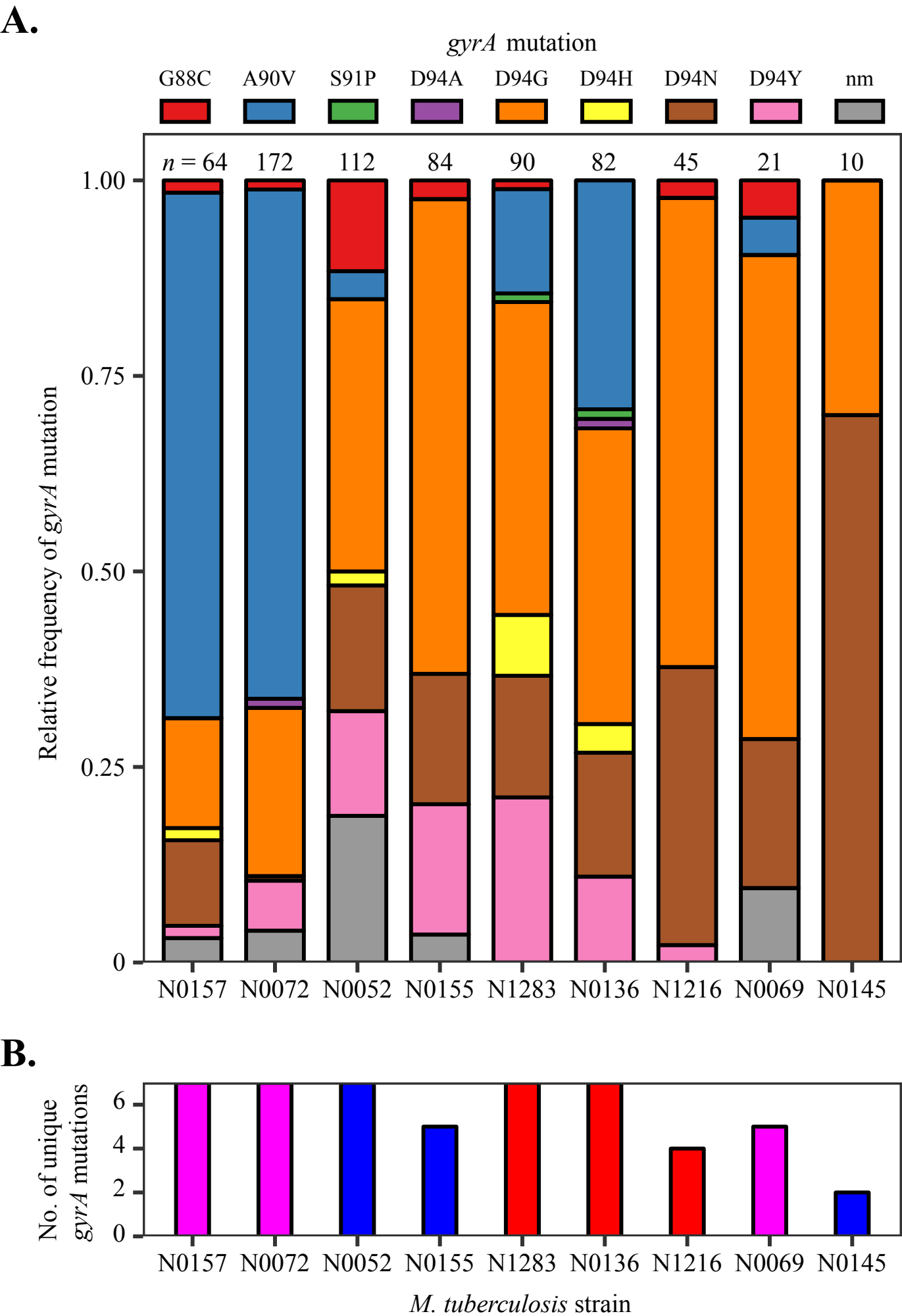
A.
gyrA mutation
G88C
A90V
S91P
D94A
D94G
D94H
D94N
D94Y
nm
n = 64
172
112
84
90
82
45
21
10
1.00
0.75
0.50
0.25
0
Relative frequency of gyrA mutation
N0157
N0072
N0052
N0155
N1283
N0136
N1216
N0069
N0145
B.
No. of unique gyrA mutations
6
4
2
0
N0157
N0072
N0052
N0155
N1283
N0136
N1216
N0069
N0145
M. tuberculosis strain

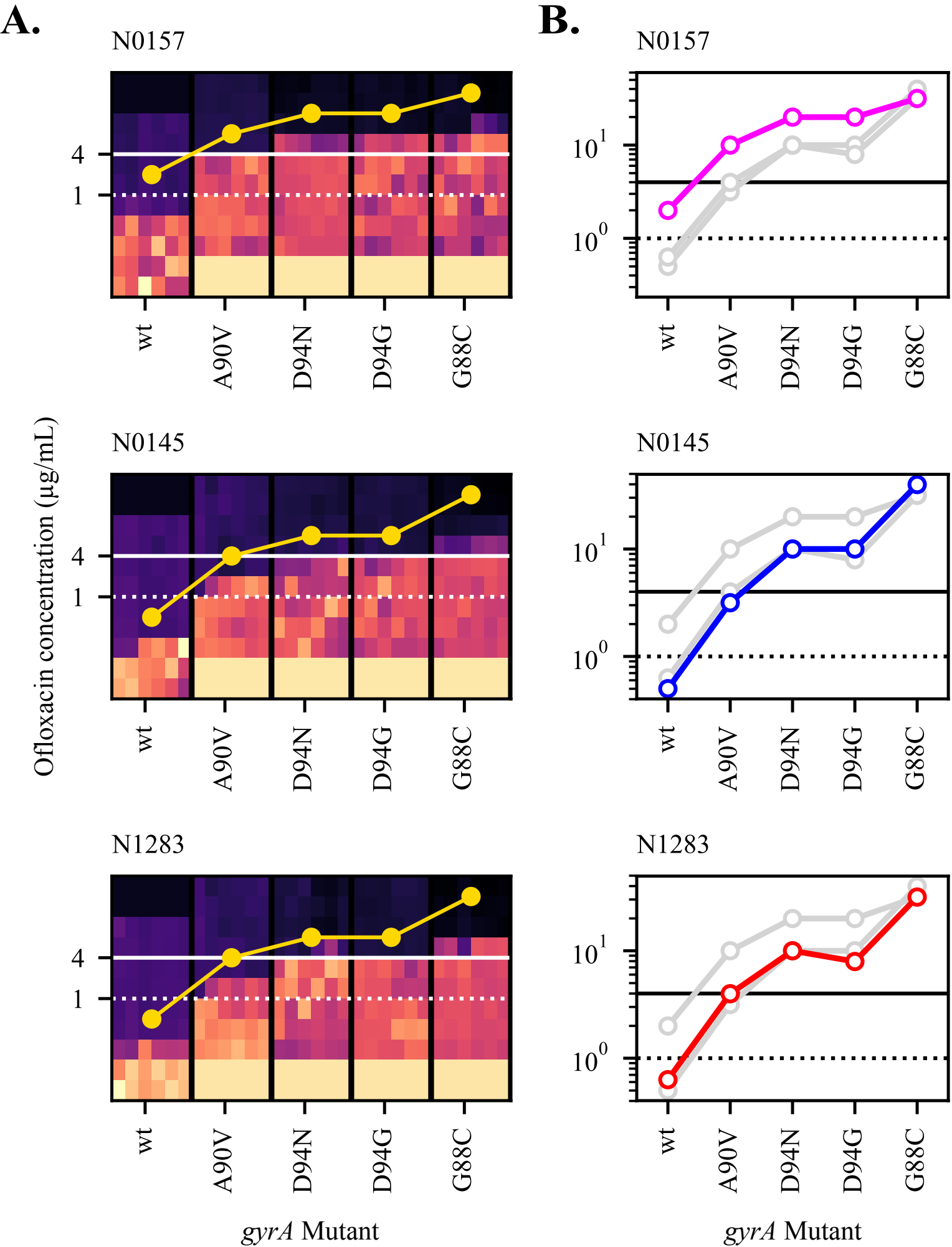
A.
B.
N0157
N0145
N1283
Ofloxacin concentration (µg/mL)
4
1
10^1
10^0
wt
A90V
D94N
D94G
G88C
gyrA Mutant

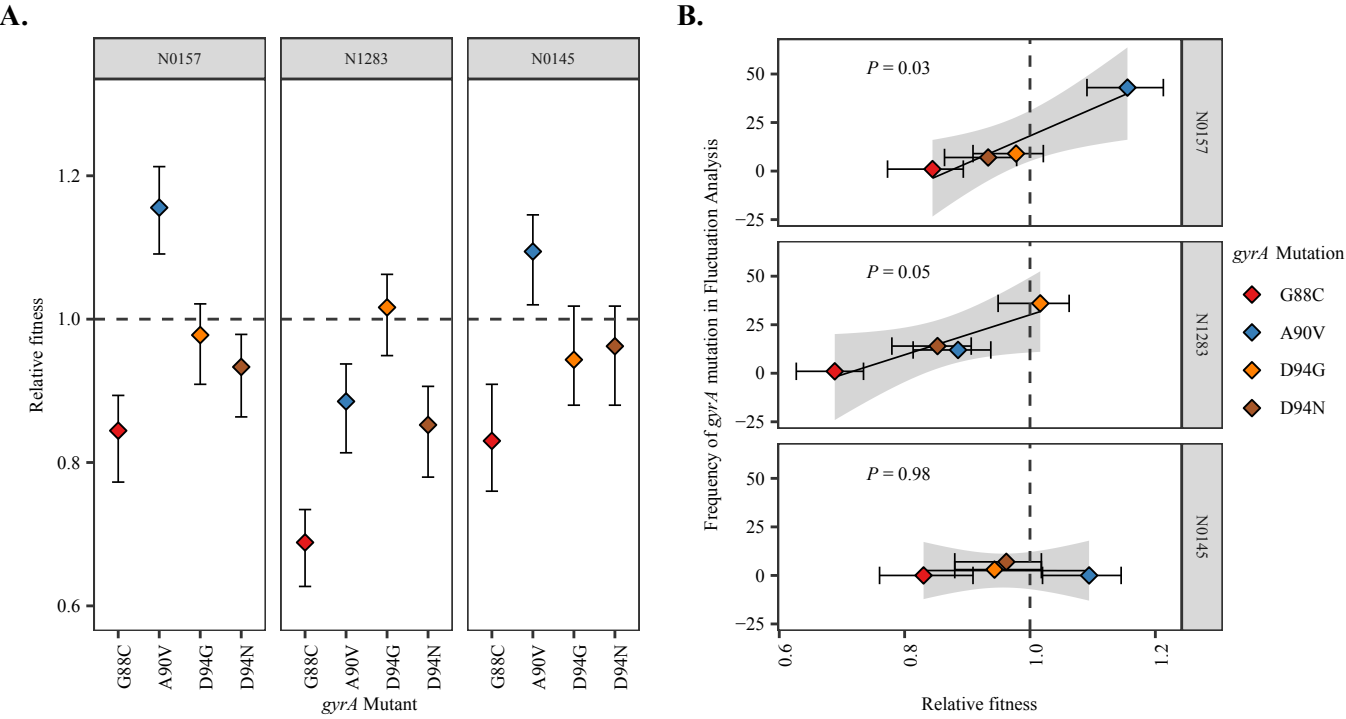
A.
N0157
N1283
N0145
Relative fitness
1.2
1.0
0.8
0.6
G88C
A90V
D94G
D94N
gyrA Mutant
B.
P = 0.03
P = 0.05
P = 0.98
Frequency of gyrA mutation in Fluctuation Analysis
50
25
0
−25
0.6
0.8
1.0
1.2
Relative fitness
gyrA Mutation
G88C
A90V
D94G
D94N

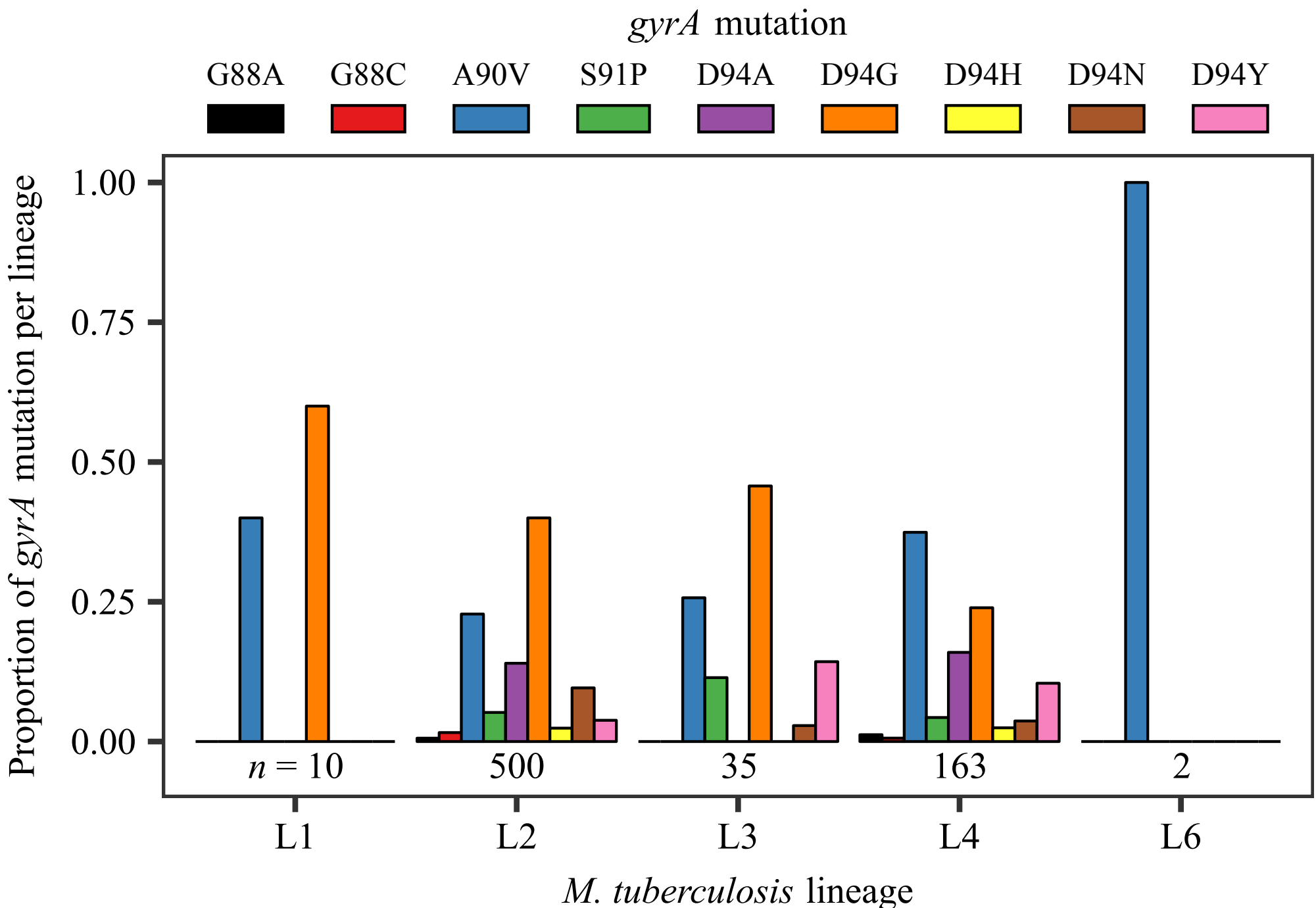
gyrA mutation
G88A
G88C
A90V
S91P
D94A
D94G
D94H
D94N
D94Y
Proportion of gyrA mutation per lineage
1.00
0.75
0.50
0.25
0.00
n = 10
500
35
163
2
L1
L2
L3
L4
L6
M. tuberculosis lineage

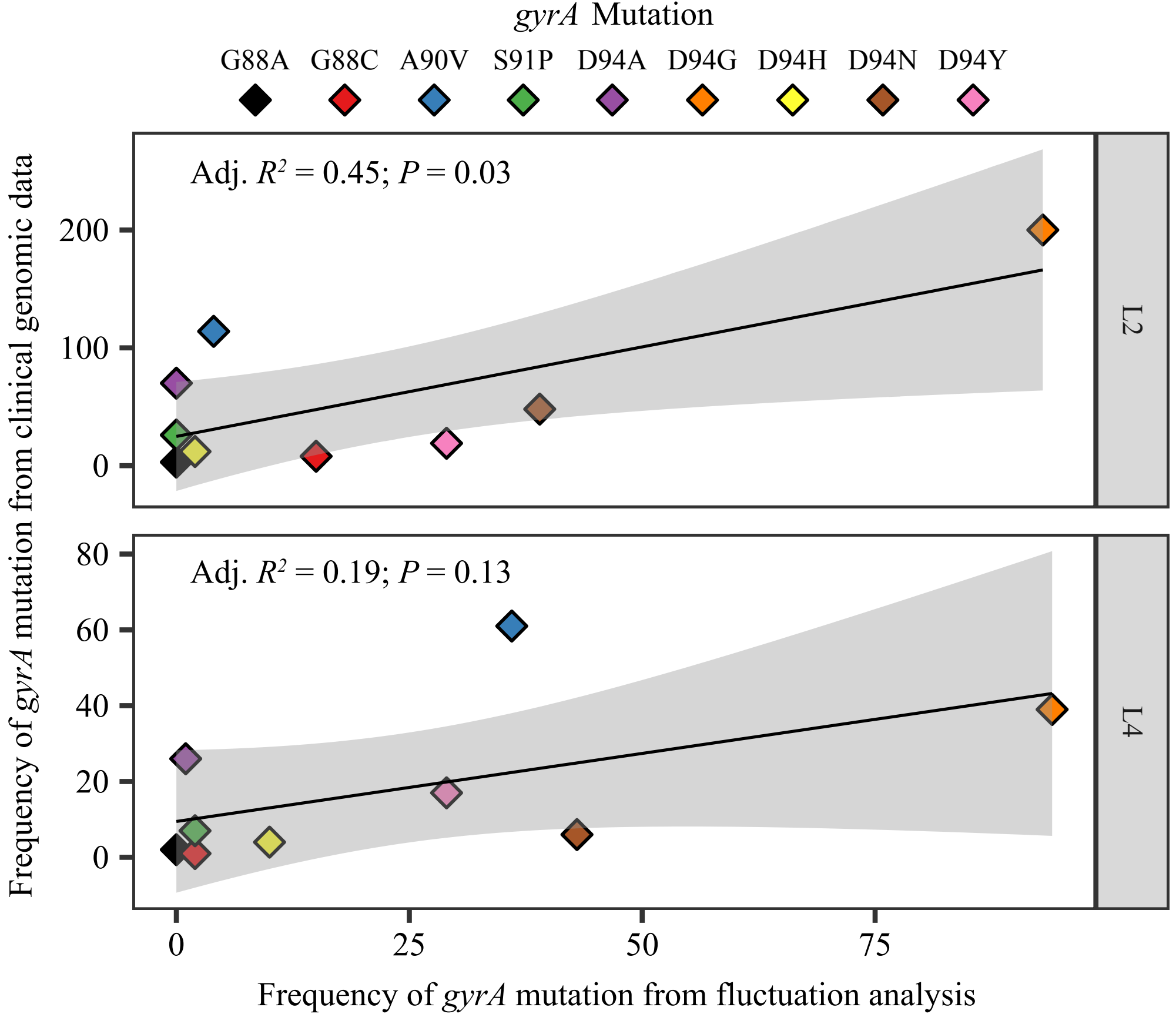
gyrA Mutation
G88A
G88C
A90V
S91P
D94A
D94G
D94H
D94N
D94Y
Adj. $R^2 = 0.45$; $P = 0.03$
Adj. $R^2 = 0.19$; $P = 0.13$
L2
L4
Frequency of gyrA mutation from clinical genomic data
Frequency of gyrA mutation from fluctuation analysis
0
25
50
75
0
100
200
0
20
40
60
80